Models for Platinum−Rhenium Bimetallic Catalysts: Sulfidation of Pt_3Re Clusters

Leijun Hao, Jianliang Xiao, Jagadese J. Vittal, and Richard J. Puddephatt*

Department of Chemistry, University of Western Ontario, London, Canada N6A 5B7

Received December 17, 1996[⊗]

Sulfidation of platinum-rhenium cluster complexes has been studied as a model for sulfidation of bimetallic Pt−Re/Al_2O_3 catalysts used in petroleum re-forming. Sulfidation of $[Pt_3\{Re(CO)_3\}(\mu\text{-dppm})_3][PF_6]$ (**1**[PF_6]; dppm = $Ph_2PCH_2PPh_2$) using propylene sulfide as reagent gives the clusters $[Pt_3\{Re(CO)_3S\}(\mu\text{-dppm})_3][PF_6]$, (**2**[$PF_6$]) and then $[Pt_3\{Re(CO)_3\}(\mu_3\text{-S})_2(\mu\text{-dppm})_3][PF_6]$ (**3**[PF_6]). Similar sulfidation of the oxo clusters $[Pt_3\{Re(CO)_3\}(\mu_3\text{-O})(\mu\text{-dppm})_3][PF_6]$, $[Pt_3\{Re(CO)_3\}(\mu_3\text{-O})_2(\mu\text{-dppm})_3][PF_6]$, and $[Pt_3(ReO_3)(\mu\text{-dppm})_3][PF_6]$ gives the oxo−sulfido clusters $[Pt_3\{Re(CO)_3\}(\mu_3\text{-O})(\mu_3\text{-S})(\mu\text{-dppm})_3][PF_6]$ (**4**[PF_6]), $[Pt_3\{Re(CO)_3\}(\mu_3\text{-O})_2(\mu_3\text{-S})(\mu\text{-dppm})_3][PF_6]$ (**5**[PF_6]), and $[Pt_3(ReO_3)(\mu_3\text{-S})_2(\mu\text{-dppm})_3][PF_6]$ (**6**[PF_6]), respectively. Oxidation of the sulfido clusters **2** and **3** by Me_3NO or H_2O_2 gave the oxo-sulfido clusters $[Pt_3\{Re(CO)_3S\}(\mu_3\text{-O})(\mu\text{-dppm})_3][PF_6]$(**7**[$PF_6$]) and $[Pt_3\{Re(CO)_3\}(\mu_3\text{-O})(\mu_3\text{-S})_2(\mu\text{-dppm})_3][PF_6]$ (**8**[PF_6]), respectively. The clusters **3**−**5** have been characterized crystallographically; addition of each μ_3-O or μ_3-S group leads to a decrease in metal−metal bonding in the cluster complexes.

Introduction

Supported bimetallic catalysts, of which Pt−Re on alumina is a prime example, are important in selective re-forming of petroleum. There is much evidence that the active catalyst contains small particles of Pt−Re alloy, perhaps bound to the oxide support through Re−O bonds. In industrial practice, the supported Pt−Re catalyst is sulfided before use.[1] During sulfidation, it is thought that surface rhenium atoms are converted to ReS groups and the rhenium centers are then deactivated. The ReS units then act as an inert diluent and serve to reduce the size of local ensembles of platinum atoms. In turn, this reduces hydrogenolysis of alkanes, since this reaction requires several adjacent, active platinum atoms. Hence, the catalysts are more selective for the desirable dehydrocyclization and isomerization reactions which increase the octane rating of the petroleum. It is also thought that adjacent rhenium atoms decrease the strength of PtS binding and so allow reversible binding of sulfur in these positions. Overall, only about 10% of surface platinum atoms are irreversibly sulfided on the Pt−Re catalyst particles. The theory is based mostly on catalytic properties, but there is also some direct evidence for selective sulfidation of rhenium.[1,2] A schematic illustration of Pt−Re and sulfided Pt−Re catalysts is shown in Figure 1.

It has been shown that the coordinatively unsaturated cluster cation $[Pt_3\{Re(CO)_3\}(\mu\text{-dppm})_3]^+$, (**1**; dppm = $Ph_2PCH_2PPh_2$)[3] can model some aspects of the bimetallic Pt−Re catalysts. Cluster **1** is remarkably versatile in binding additional ligands, and examples of ligand addition to rhenium only, to platinum only, or at a Pt_2-Re face are known.[4,5] Of particular relevance to the present work are oxygen atom additions which occur according to Scheme 1.[5] Initial addition occurs at Pt_2-Re faces with progressive loss of metal−metal bonding as more oxygen atoms are added. Under forcing conditions, conversion of the $Re(CO)_3$ group to $Re(=O)_3$ can occur and eventual oxidation to perrhenate may be observed.[5] It was of interest to determine if sulfur atom additions to **1** might occur in an analogous way and serve as a model for the sulfidation of bimetallic Pt−Re catalysts. Fortunately, this was successful and the results, some of which have been communicated in preliminary form,[6] are given below. Some relevant chemistry of platinum−rhenium complexes has been published recently.[7,8]

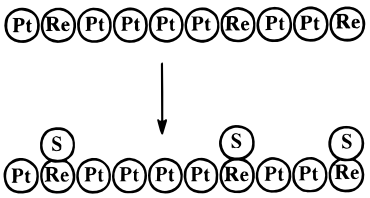

Figure 1. Proposed surface structures of PtRe cluster particles shown in simplified form before and after sulfidation.

[⊗] Abstract published in *Advance ACS Abstracts,* April 15, 1997.

(1) (a) Biswas, J.; Bickle, G. M.; Gray, P. G.; Do, D. D.; Barbier, J. *Catal. Rev.−Sci. Eng.* **1988**, *30*, 161. (b) Parera, J. M.; Figoli, N. S. *Catalysis* **1992**, *9*, 64. (c) Michel, C. G.; Bambrick, W. E. *Fuel Process. Technol.* **1993**, *35*, 159.

(2) (a) Biloen, P.; Helle, J. N.; Verbeek, H.; Dautzenberg, F. M.; Sachtler, W. M. H. *J. Catal.* **1980**, *63*, 112. (b) Xiao, J.; Puddephatt, R. J. *Coord. Chem. Rev.* **1995**, *143*, 457.

(3) Xiao, J.; Kristof, E.; Vittal, J. J.; Puddephatt, R. J. *J. Organomet. Chem.* **1995**, *490*, 1.

(4) (a) Xiao, J.; Hao, L; Puddephatt, R. J.; Manojlovic-Muir, L.; Muir, K. W.; Torabi, A. *Organometallics* **1995**, *14*, 2194. (b) Xiao, J.; Hao, L.; Puddephatt, R. J.; Manojlovic-Muir, L.; Muir, K. W.; Torabi, A. *Organometallics* **1995**, *14*, 4183.

(5) (a) Xiao, J.; Vittal, J. J.; Puddephatt, R. J.; Manojlovic-Muir, L.; Muir, K. W. *J. Am. Chem. Soc.* **1993**, *115*, 7882. (b) Xiao, J.; Puddephatt, R. J.; Manojlovic-Muir, L.; Muir, K. W.; Torabi, A. *J. Am. Chem. Soc.* **1994**, *116*, 1129. (c) Xiao, J.; Hao, L.; Puddephatt, R. J.; Manojlovic-Muir, L.; Muir, K. W. *J. Am. Chem. Soc.* **1995**, *117*, 6316.

(6) (a) Hao, L.; Xiao, J.; Vittal, J. J.; Puddephatt, R. J. *J. Chem. Soc., Chem. Commun.* **1994**, 2183. (b) Hao, L.; Xiao, J.; Vittal, J. J.; Puddephatt, R. J. *Angew. Chem., Int. Ed. Engl.* **1995**, *34*, 346.

(7) (a) Mague, J. T. *Inorg. Chem.* **1994**, *33*, 4261. (b) Fukuoka, A.; Minami, Y.; Nakajima, N.; Hirano, M.; Komiya, S. *J. Mol. Catal. A: Chem.* **1996**, *107*, 323.

S0276-7333(96)01061-8 CCC: $14.00

Scheme 1

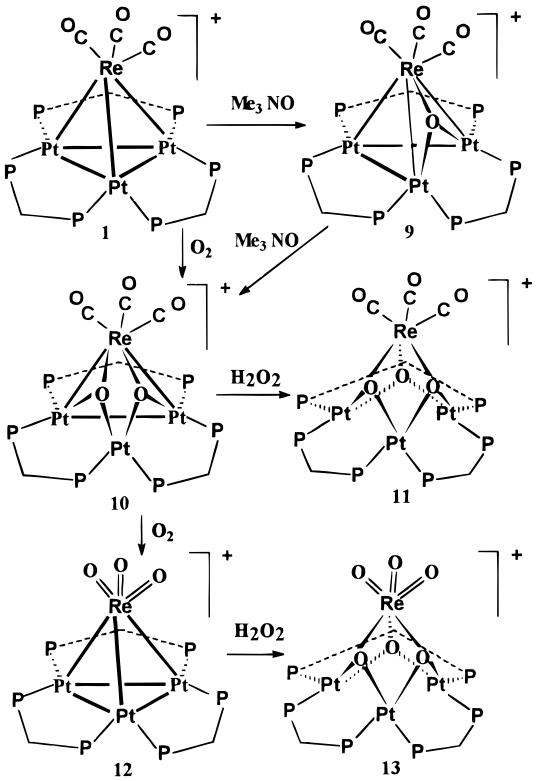

Scheme 2

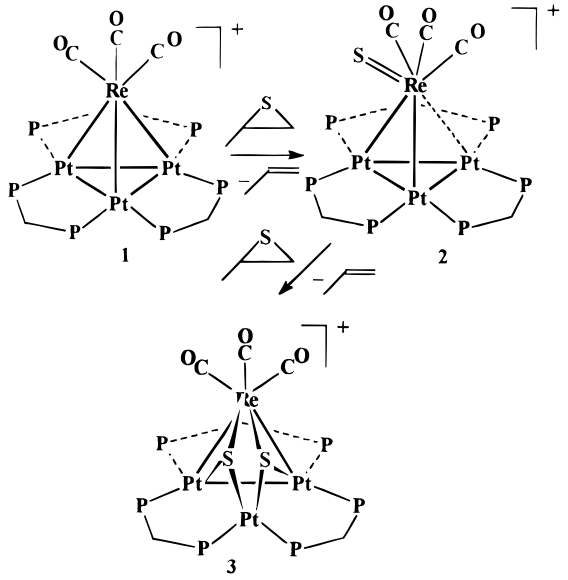

Results

Sulfidation of $[Pt_3\{Re(CO)_3\}(\mu\text{-dppm})_3][PF_6]$ (1) with Formation of the Clusters $[Pt_3\{Re(CO)_3S\}(\mu\text{-dppm})_3][PF_6]$ (2[PF_6]) and $[Pt_3\{Re(CO)_3\}(\mu_3\text{-S})_2(\mu\text{-dppm})_3][PF_6]$ (3[PF_6]). The reaction of $[Pt_3\{Re(CO)_3\}(\mu\text{-dppm})_3][PF_6]$ (**1**[PF_6]) with two molar equiv of propylene sulfide proceeded to give the red disulfido complex $[Pt_3\{Re(CO)_3\}(\mu_3\text{-S})_2(\mu\text{-dppm})_3][PF_6]$ (**3**[PF_6]) with the evolution of propene (Scheme 2).[9] The disulfido cluster **3** is analogous to the known dioxo complex $[Pt_3\{Re(CO)_3\}(\mu_3\text{-O})_2(\mu\text{-dppm})_3][PF_6]$ (**10**[PF_6])[5] and is indefinitely stable in air at room temperature. Complex **3** is sparingly soluble in acetone and precipitated as red prismatic crystals when the reaction was carried out in this solvent; **3** is more soluble in dichloromethane solution. Cluster **3** failed to react with excess propylene sulfide to give a trisulfido derivative. The reaction of **1** with propylene sulfide was approximately first order in the concentration of propylene sulfide; with a 6-fold excess of propylene sulfide the reaction was complete in 30 min at room temperature.

Interestingly, the formation of the disulfido cluster **3** proceeded via an intermediate species, identified as the red-brown monosulfide cluster $[Pt_3\{Re(CO)_3S\}(\mu\text{-dppm})_3][PF_6]$ (**2**[PF_6]) (Scheme 2). However, complex **2** is not the analog of the monooxo cluster $[Pt_3\{Re(CO)_3\}(\mu_3\text{-O})(\mu\text{-dppm})_3][PF_6]$ (**9**[PF_6]) (Scheme 1) but is tentatively suggested to contain a terminal Re═S bond. Complex **2** was formed immediately after the addition of propylene sulfide to a solution of **1**, and propene was evolved as detected by ^1H NMR. However, its further transformation to the disulfido cluster **3** took several hours to complete, as monitored by ^1H and ^{31}P NMR spectroscopy. If only 1 equiv of propylene sulfide was used, **2** was the dominant product with the presence of trace amounts of **1** and **3**. Complex **2** could be obtained in pure form by immediately precipitating the product by the addition of hexane, but attempts to grow single crystals were unsuccessful due to the limited stability of **2** in solution. In one experiment, a solution of complex **2** in CD_2Cl_2 under an atmosphere of dry nitrogen was shown to decompose completely over a period of 5 days at room temperature to give a complex mixture of products. When a solution of complex **2** in acetone was heated to 50 °C, complete decomposition took place in *ca.* 10 min. In the presence of air, a solution of complex **2** in CD_2Cl_2 decomposed completely in 1 day to give the dioxo complex $[Pt_3\{Re(CO)_3\}(\mu_3\text{-O})_2(\mu\text{-dppm})_3][PF_6]$ (**10**[PF_6]).[5]

Mixed Oxo−Sulfido Clusters by Sulfidation of Oxo Clusters. Sulfur poisoning is a very important process in industrial catalytic re-forming and is usually applied to the oxide-supported bimetallic catalysts such as $Pt-Re/Al_2O_3$.[1,2] Since many believe that such catalysts contain Re−O linkages, it was of interest to study sulfidation of the oxo clusters **9**, **10**, and **12** (Scheme 1)[5] as a relevant model system.

The oxo clusters **9** and **10** each added one sulfur atom on reaction with propylene sulfide to give the red monooxo monosulfido cluster $[Pt_3\{Re(CO)_3\}(\mu_3\text{-O})(\mu_3\text{-S})(\mu\text{-dppm})_3][PF_6]$ (**4**[PF_6]) and the yellow dioxo monosulfido cluster $[Pt_3\{Re(CO)_3\}(\mu_3\text{-O})_2(\mu_3\text{-S})(\mu\text{-dppm})_3][PF_6]$ (**5**[PF_6]), respectively, with the evolution of propene, as shown in eqs 1 and 2. Each reaction took *ca.* 4 h to reach completion, using a 10-fold excess of propylene sulfide, and no intermediate was detected in either case, as monitored by ^1H and ^{31}P NMR spectroscopy. The complexes **4** and **5** are air-stable both in the solid state and in solution.

The reaction of trioxo cluster $[Pt_3\{ReO_3\}(\mu\text{-dppm})_3]^+$ (**12**)[5] with excess propylene sulfide afforded the new

(8) (a) Ciani, G.; Moret, M.; Sironi, A.; Antognazza, P.; Beringhelli, T.; D'Alfonso, G.; Pergola, R. D.; Minoja, A. *J. Chem. Soc., Chem. Commun.* **1991**, 1255. (b) Xu, Z.; Kawi, S.; Rheingold, A. L.; Gates, B. C. *Inorg. Chem.* **1994**, *33*, 4415.

(9) Vahrenkamp, H. *Angew. Chem., Int. Ed. Engl.* **1975**, *14*, 322.

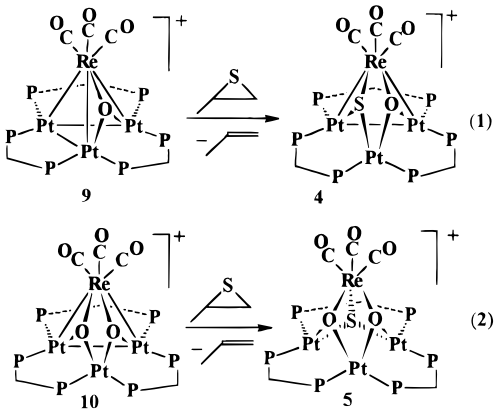

cluster $[Pt_3\{ReO_3\}(\mu_3\text{-}S)_2(\mu\text{-dppm})_3]^+$ (**6**) with the evolution of propene (eq 3). The reaction took ca. 16 h to

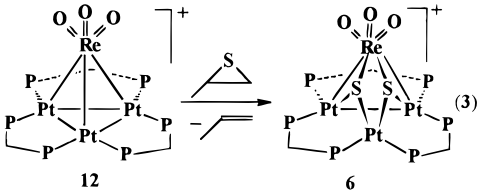

reach completion, as monitored by ^{31}P NMR spectroscopy. This reaction is analogous to that of cluster **1** with propylene sulfide to form the disulfido cluster **3**. An intermediate was also observed in this reaction, as monitored by ^{31}P NMR spectroscopy, with two broad resonances at δ 23.6 and −7.4 in the ratio 1:2. Efforts were made to isolate and to identify the intermediate, but these have not been successful so far due to its thermal instability.

Mixed Oxo−Sulfido Clusters by Oxygen Atom Addition to Sulfido Clusters. Reaction of the cluster $[Pt_3\{Re(CO)_3S\}(\mu\text{-dppm})_3][PF_6]$ (**2**$[PF_6]$) with 1 equiv of hydrated Me_3NO proceeded to give the new red cluster **7**,$[PF_6]$ which is proposed to have the structure $[Pt_3\{Re(CO)_3S\}(\mu_3\text{-}O)(\mu\text{-dppm})_3][PF_6]$, according to eq 4. Clus-

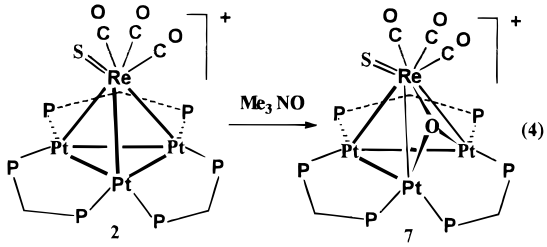

ter **7** was characterized spectroscopically, and its spectra are very different from those of the isomeric cluster **4**. Well-shaped red prismatic crystals of **7** could be obtained from CH_2Cl_2/hexane but were not of X-ray quality. Attempts to interconvert clusters **4** and **7** by refluxing in tetrahydrofuran or benzene solution were unsuccessful; both clusters were stable under these conditions, and more forcing conditions led to general decomposition.

The disulfido cluster **3** failed to react with Me_3NO, but it did react slowly with the stronger oxidant H_2O_2, as shown in eq 5. In a typical experiment, the reaction of **3** with excess H_2O_2 in CH_2Cl_2 solution, as monitored by ^{31}P NMR spectroscopy, took about 1 day to reach completion and the yellow product $[Pt_3\{Re(CO)_3\}(\mu_3\text{-}O)$-

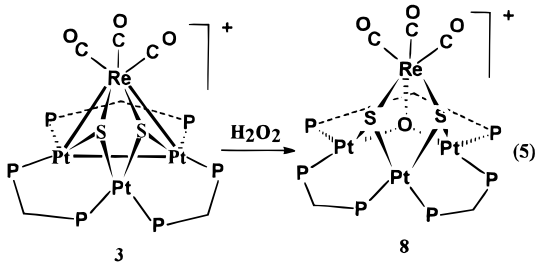

$(\mu_3\text{-}S)_2(\mu\text{-dppm})_3][PF_6]$ (**8**$[PF_6]$) was formed in about 50% yield, with the other 50% giving the dioxide of dppm and uncharacterized material. Cluster **3** has low reactivity with other reagents also. For example, no reaction occurred on treatment with phosphine or phosphite ligands, and no CO exchange occurred on reaction with ^{13}CO, whereas the analogous dioxo cluster **10** does react under these conditions to give CO substitution or exchange.[5]

Structures of the Sulfido Clusters 3−5. The structures of the clusters **3**−**5** are shown in Figures 2−4, and selected bond distances and angles are given in Tables 1−3. The complexes are isomorphous, and the cell volume follows the trend **3** > **5** > **4**, reflecting the core expansion with larger substituents (Table 4). The molecular ion **3** contains a cluster of one rhenium and three platinum atoms with distorted-tetrahedral geometry. The three platinum atoms define an approximately isosceles triangle with each edge bridged by a μ-dppm ligand. The atoms Pt(3), Re, and C(10) define an approximate mirror plane; the most obvious distortions from C_s symmetry arise from the orientations of the phenyl rings. The incorporation of two μ_3-S bridging atoms is accompanied by a significant lengthening of all the metal−metal distances compared to those in **1** (Table 1). The distances Pt(3)···Re, Pt(3)···Pt(1), and Pt(3)···Pt(2) at 3.625(2), 3.270(2), and 3.213(2) Å, respectively, are too long for significant bonding, and so Pt(3) appears to have square-planar *cis*-PtP_2S_2 coordination only, with no metal−metal bonding. The metal−metal distances Pt(1)−Pt(2) = 3.038(2) Å and Pt(1)−Re and Pt(2)−Re = 2.946(2) and 3.002(2) Å, respectively, are also longer than the average Pt−Pt and Pt−Re distances of 2.602 and 2.726 Å, respectively, in **1**, indicating weak metal−metal bonding within the Pt(1)Pt(2)Re triangle in **3**. Furthermore, in comparison to Pt(1)−Pt(2) = 2.826(1) Å and Pt(1)−Re and Pt(2)−Re = 2.834(1) and 2.854(2) Å, respectively, in $[Pt_3\{Re(CO)_3\}(\mu_3\text{-}O)_2(\mu\text{-dppm})_3]^+$ (**10**),[5] in which two μ_3-O ligands instead of the two μ_3-S ligands cap the open Pt_2Re triangular faces, the metal−metal distances Pt(1)−Pt(2), Pt(1)−Re, and Pt(2)−Re in **3** also appear to be long. The expansion of the metal tetrahedron in **3** compared to that in **10** is attributed to the larger size of the sulfido compared to the oxo ligands.[10,11] The triply bridging sulfido ligands span the two open Pt_2Re trianglar faces in a nearly symmetrical fashion. The platinum−sulfur distances span the range 2.322(8)−2.356(7) Å and are similar to those Pt−S bond distances observed in other sulfido-bridged platinum-containing clusters.[12] The

(10) Mingos, D. M. P.; Wardle, R. W. M. *Transition Met. Chem.* **1985**, *10*, 441.
(11) Evans, D. G.; Hughes, G. R.; Mingos, D. M. P.; Bassett, J.-M.; Welch, A. J. *J. Chem. Soc., Chem. Commun.* **1980**, 1255.

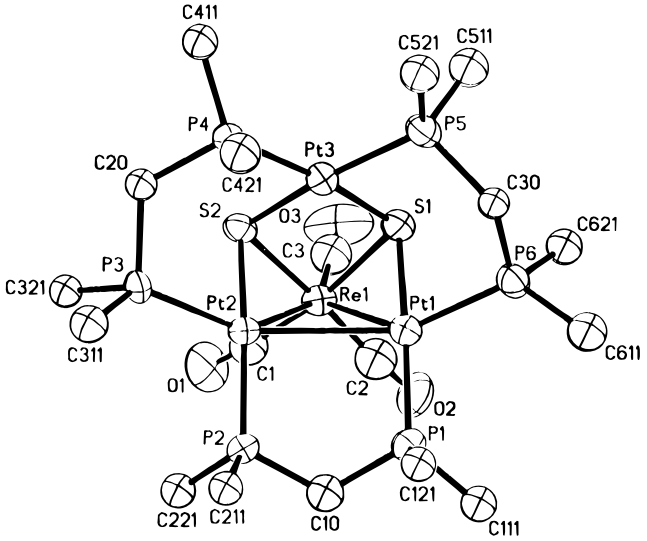

Figure 2. View of the structure of the cluster cation **3**. Only the *ipso* carbon atoms of the phenyl groups are shown.

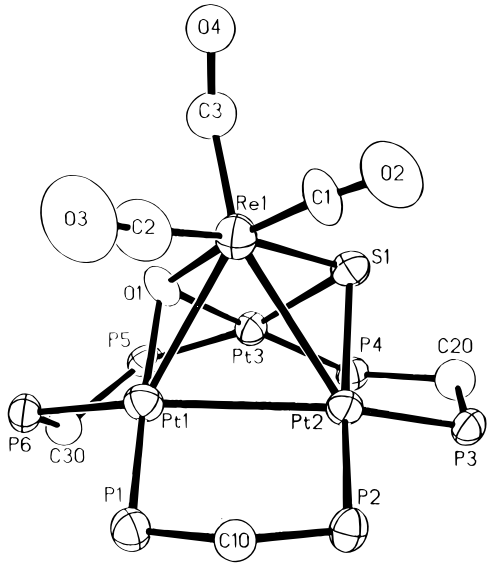

Figure 3. View of the structure of the cluster cation **4**. Phenyl groups are omitted for clarity.

sulfur−sulfur distance of 3.088 Å indicates no S−S bonding.[13,14] The Re−S distances Re−S(1) = 2.463(8) Å and Re−S(2) = 2.470(8) Å are normal in comparison to other sulfido-bridged rhenium-containing clusters.[15,16] The Pt_3S_2 ring displays an envelope conformation characterized by an S(1)−Pt(1)−Pt(2)−S(2) torsion angle of less than 3°, with the Pt(3) flap directed away from the Re atom. The Pt−P distances Pt(2)−P(3) = 2.290(8) Å and Pt(1)−P(6) = 2.300(8) Å, which are *trans* to a metal−metal bond, are longer than those (2.256(8)−2.286(8) Å) *trans* to a sulfur atom. In the dioxo cluster **10**, the Pt−P bond distances trans to the metal−metal bonds are very similar, while the Pt−P bond lengths

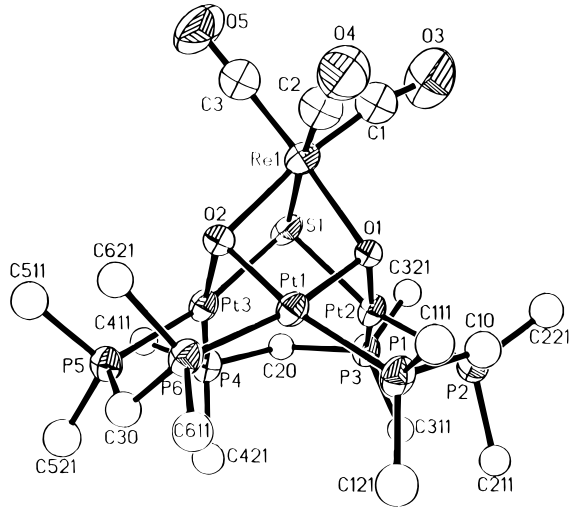

Figure 4. View of the structure of the cluster cation **5**. Only the *ipso* carbon atoms of the phenyl groups are shown.

Table 1. Selected Bond Lengths (Å) and Angles (deg) for 3

Pt(1)−Pt(2)	3.038(2)	Pt(1)−Re(1)	2.946(2)
Pt(1)−S(1)	2.350(8)	Pt(1)−P(1)	2.256(8)
Pt(1)−P(6)	2.300(8)	Pt(2)−Re(1)	3.002(2)
Pt(2)−S(2)	2.356(7)	Pt(2)−P(2)	2.261(7)
Pt(2)−P(3)	2.290(8)	Pt(3)−S(1)	2.322(8)
Pt(3)−S(2)	2.352(8)	Pt(3)−P(4)	2.281(8)
Pt(3)−P(5)	2.286(8)	Re(1)−S(1)	2.463(8)
Re(1)−S(2)	2.470(8)	Re(1)−C(1)	1.91(3)
Re(1)−C(2)	1.82(4)	Re(1)−C(3)	1.80(4)
Pt(2)−Pt(1)−Re(1)	60.2(1)	Pt(2)−Pt(1)−S(1)	90.1(2)
Re(1)−Pt(1)−S(1)	54.0(2)	Pt(2)−Pt(1)−P(1)	88.9(2)
Re(1)−Pt(1)−P(1)	117.8(2)	S(1)−Pt(1)−P(1)	170.5(3)
Pt(2)−Pt(1)−P(6)	145.2(2)	Re(1)−Pt(1)−P(6)	132.2(2)
S(1)−Pt(1)−P(6)	81.3(3)	P(1)−Pt(1)−P(6)	104.7(3)
Pt(1)−Pt(2)−Pt(3)	63.0(1)	Pt(1)−Pt(2)−Re(1)	58.4(1)
Pt(3)−Pt(2)−Re(1)	71.3(1)	Pt(1)−Pt(2)−S(2)	90.9(2)
Pt(3)−Pt(2)−S(2)	46.9(2)	Re(1)−Pt(2)−S(2)	53.2(2)
Pt(1)−Pt(2)−P(2)	91.0(2)	Pt(3)−Pt(2)−P(2)	146.1(2)
Re(1)−Pt(2)−P(2)	114.9(2)	S(2)−Pt(2)−P(2)	163.4(3)
Pt(1)−Pt(2)−P(3)	148.4(2)	Pt(3)−Pt(2)−P(3)	91.5(2)
Re(1)−Pt(2)−P(3)	133.6(2)	S(2)−Pt(2)−P(3)	83.2(3)
P(2)−Pt(2)−P(3)	103.3(3)	Pt(2)−Pt(3)−S(1)	86.4(2)
Pt(2)−Pt(3)−S(2)	47.0(2)	S(1)−Pt(3)−S(2)	82.5(3)
Pt(2)−Pt(3)−P(4)	87.4(2)	S(1)−Pt(3)−P(4)	172.3(3)
S(2)−Pt(3)−P(4)	89.9(3)	Pt(2)−Pt(3)−P(5)	134.9(2)
S(1)−Pt(3)−P(5)	86.6(3)	S(2)−Pt(3)−P(5)	168.9(3)
P(4)−Pt(3)−P(5)	100.9(3)	Pt(1)−Re(1)−Pt(2)	61.4(1)
Pt(1)−Re(1)−S(1)	50.5(2)	Pt(2)−Re(1)−S(1)	88.8(2)
Pt(1)−Re(1)−S(2)	90.9(2)	Pt(2)−Re(1)−S(2)	49.8(2)
S(1)−Re(1)−S(2)	77.4(3)	Pt(1)−Re(1)−C(1)	131.6(11)
Pt(2)−Re(1)−C(1)	85.1(11)	S(1)−Re(1)−C(1)	169.8(11)
S(2)−Re(1)−C(1)	92.5(11)	Pt(1)−Re(1)−C(2)	80.0(13)
Pt(2)−Re(1)−C(2)	119.9(13)	S(1)−Re(1)−C(2)	100.8(12)
S(2)−Re(1)−C(2)	169.3(13)	C(1)−Re(1)−C(2)	89.4(16)
Pt(1)−Re(1)−C(3)	134.4(12)	Pt(2)−Re(1)−C(3)	152.6(12)
S(1)−Re(1)−C(3)	90.2(12)	S(2)−Re(1)−C(3)	103.4(12)
C(1)−Re(1)−C(3)	91.4(16)	C(2)−Re(1)−C(3)	87.1(18)
Pt(1)−S(1)−Pt(3)	88.8(3)	Pt(1)−S(1)−Re(1)	75.4(2)
Pt(3)−S(1)−Re(1)	98.4(3)	Pt(2)−S(2)−Pt(3)	86.1(3)
Pt(2)−S(2)−Re(1)	76.9(2)	Pt(3)−S(2)−Re(1)	97.5(3)
Re(1)−C(1)−O(1)	171(3)	Re(1)−C(2)−O(2)	176(3)
Re(1)−C(3)−O(3)	179(3)		

(12) (a) Douglas, G.; Jennings, M. C.; Manojlovic-Muir, L.; Puddephatt, R. J. *Inorg. Chem.* **1988**, *27*, 4516. (b) Jennings, M. C.; Payne, N. C.; Puddephatt, R. J. *J. Chem. Soc., Chem. Commun.* **1986**, 1809. (c) Jennings, M. C.; Payne, N. C.; Puddephatt, R. J. *Inorg. Chem.* **1987**, *26*, 3776. (d) Bushnell, G. W.; Dixon, K. R.; Ono, R.; Pidcock, A. *Can. J. Chem.* **1984**, *62*, 696. (e) Ewing, P.; Farrugia, L. J. *J. Organomet. Chem.* **1989**, *373*, 256. (f) Adams, R. D.; Hor, A. T. S. *Inorg. Chem.* **1984**, *23*, 4723. (g) Adams, R. D.; Hor, A. T. S.; Horvath, I. T. *Inorg. Chem.* **1984**, *23*, 4733. (h) Adams, R. D.; Horvath, I. T.; Wang, S. *Inorg. Chem.* **1986**, *25*, 1617.

(13) (a) Muller, A.; Jaegermann, W.; Enemark, J. H. *Coord. Chem. Rev.* **1982**, *46*, 245. (b) Elder, R. C.; Trkula, M. *Inorg. Chem.* **1977**, *16*, 1048. (c) Wei, C. H.; Dahl, L. F. *Inorg. Chem.* **1965**, *4*, 1.

(14) Stevenson, D. L.; Magnuson, V. R.; Dahl, L. F. *J. Am. Chem. Soc.* **1967**, *89*, 3727.

(15) Eremenko, I. L.; Berke, H.; Kolobkov, B. I.; Novotortsev, V. M. *Organometallics* **1994**, *13*, 244.

(16) (a) Antognazza, P.; Beringhelli, T.; D'Alfonso, G.; Minoja, A.; Ciani, G.; Moret, M.; Sironi, A. *Organometallics* **1992**, *11*, 1777. (b) Ciani, G.; Moret, M.; Sironi, A.; Beringhelli, T.; D'Alfonso, G.; Pergola, R. D. *J. Chem. Soc., Chem. Commun.* **1990**, 1668.

Table 2. Selected Bond Lengths (Å) and Angles (deg) for 4

Pt(1)−O(1)	2.07(1)	Pt(1)−P(1)	2.237(6)
Pt(1)−P(6)	2.292(6)	Pt(1)−Re(1)	2.882(2)
Pt(1)−Pt(2)	2.957(1)	Pt(1)−Pt(3)	3.152(1)
Pt(2)−P(2)	2.264(6)	Pt(2)−P(3)	2.289(6)
Pt(2)−S(1)	2.358(6)	Pt(2)−Re(1)	3.051(1)
Pt(2)−Pt(3)	3.115(1)	Pt(3)−O(1)	2.09(1)
Pt(3)−P(4)	2.242(6)	Pt(3)−P(5)	2.280(6)
Pt(3)−S(1)	2.320(6)	Re(1)−C(3)	1.83(3)
Re(1)−C(1)	1.85(3)	Re(1)−C(2)	1.88(3)
Re(1)−O(1)	2.16(1)	Re(1)−S(1)	2.439(6)
O(1)−Pt(1)−P(1)	170.6(4)	O(1)−Pt(1)−P(6)	83.5(4)
P(1)−Pt(1)−P(6)	104.0(2)	O(1)−Pt(1)−Re(1)	48.3(4)
P(1)−Pt(1)−Re(1)	122.5(2)	P(6)−Pt(1)−Re(1)	126.3(2)
O(1)−Pt(1)−Pt(2)	85.4(4)	P(1)−Pt(1)−Pt(2)	91.0(2)
P(6)−Pt(1)−Pt(2)	146.6(2)	Re(1)−Pt(1)−Pt(2)	62.98(3)
O(1)−Pt(1)−Pt(3)	40.9(4)	P(1)−Pt(1)−Pt(3)	142.7(2)
P(6)−Pt(1)−Pt(3)	90.7(2)	Re(1)−Pt(1)−Pt(3)	69.03(3)
Pt(2)−Pt(1)−Pt(3)	61.22(3)	P(2)−Pt(2)−P(3)	104.1(2)
P(2)−Pt(2)−S(1)	162.7(2)	P(3)−Pt(2)−S(1)	82.0(2)
P(2)−Pt(2)−Pt(1)	90.8(2)	P(3)−Pt(2)−Pt(1)	148.3(2)
S(1)−Pt(2)−Pt(1)	91.9(2)	P(2)−Pt(2)−Re(1)	117.2(2)
P(3)−Pt(2)−Re(1)	132.2(2)	S(1)−Pt(2)−Re(1)	51.7(2)
Pt(1)−Pt(2)−Re(1)	57.31(3)	P(2)−Pt(2)−Pt(3)	146.0(2)
P(3)−Pt(2)−Pt(3)	91.7(2)	S(1)−Pt(2)−Pt(3)	47.7(2)
Pt(1)−Pt(2)−Pt(3)	62.47(3)	Re(1)−Pt(2)−Pt(3)	67.50(3)
O(1)−Pt(3)−P(4)	170.0(4)	O(1)−Pt(3)−P(5)	88.6(4)
P(4)−Pt(3)−P(5)	100.5(2)	O(1)−Pt(3)−S(1)	81.7(4)
P(4)−Pt(3)−S(1)	89.7(2)	P(5)−Pt(3)−S(1)	168.0(2)
O(1)−Pt(3)−Pt(2)	81.1(4)	P(4)−Pt(3)−Pt(2)	89.3(1)
P(5)−Pt(3)−Pt(2)	136.7(2)	S(1)−Pt(3)−Pt(2)	48.8(1)
O(1)−Pt(3)−Pt(1)	40.6(4)	P(4)−Pt(3)−Pt(1)	134.4(2)
P(5)−Pt(3)−Pt(1)	89.4(2)	S(1)−Pt(3)−Pt(1)	87.9(2)
Pt(2)−Pt(3)−Pt(1)	56.31(3)	C(3)−Re(1)−C(1)	89(1)
C(3)−Re(1)−C(2)	88(1)	C(1)−Re(1)−C(2)	85(1)
C(3)−Re(1)−O(1)	95(1)	C(1)−Re(1)−O(1)	171.2(9)
C(2)−Re(1)−O(1)	102.6(9)	C(3)−Re(1)−S(1)	101.7(9)
C(1)−Re(1)−S(1)	93.9(8)	C(2)−Re(1)−S(1)	170.3(9)
O(1)−Re(1)−S(1)	77.6(4)	C(3)−Re(1)−Pt(1)	135(1)
C(1)−Re(1)−Pt(1)	133.5(8)	C(2)−Re(1)−Pt(1)	81.5(9)
O(1)−Re(1)−Pt(1)	45.8(4)	S(1)−Re(1)−Pt(1)	92.1(2)
C(3)−Re(1)−Pt(2)	150.9(8)	C(1)−Re(1)−Pt(2)	91.0(9)
C(2)−Re(1)−Pt(2)	120.9(9)	O(1)−Re(1)−Pt(2)	81.7(4)
S(1)−Re(1)−Pt(2)	49.3(1)	Pt(1)−Re(1)−Pt(2)	59.72(3)
Pt(3)−S(1)−Pt(2)	83.5(2)	Pt(3)−S(1)−Re(1)	92.1(2)
Pt(2)−S(1)−Re(1)	79.0(2)	Pt(1)−O(1)−Pt(3)	98.6(6)
Pt(1)−O(1)−Re(1)	85.9(5)	Pt(3)−O(1)−Re(1)	107.7(6)
O(2)−C(1)−Re(1)	173(3)	O(3)−C(2)−Re(1)	175(3)
O(4)−C(3)−Re(1)	163(3)		
O(4A)−C(3)−Re(1)	165(3)		

(2.227(3)−2.243(3) Å) *trans* to the oxygen atom are much shorter than those *trans* to sulfur in **3**.

The structure of the cluster cation **4** is similar to those of **3** and **10**, but in this case one Pt_2Re face is capped by a μ_3-oxo ligand and one by a μ_3-sulfido ligand. Again, the distances Pt(3)···Re = 3.426(1) Å and Pt(3)···Pt(1) and Pt(3)···Pt(2) = 3.152(1) and 3.115(1) Å, respectively, are too long for significant bonding and so Pt(3) appears to have square-planar *cis*-PtP_2SO coordination with no metal−metal bonding. The metal−metal distances Pt(1)−Pt(2) = 2.957(1) Å, Pt(1)−Re = 2.882(1) Å, and Pt(2)−Re = 3.051(1) Å are also long, indicating weak metal−metal bonding within the Pt(1)Pt(2)Re triangle. The Pt(2)−Re distance is longer than the Pt(1)−Re distance, presumably due to the proximity to the larger sulfido ligand, compared to oxo bridging ligand. The Pt(1)−Pt(2) distance in **4** is longer than in **10** but shorter than that in **3**. Indeed, all the metal−metal distances in **4** fall between the corresponding distances in **3** and **10** (Table 4). The Pt−P bond distances span the range 2.237(6)−2.292(6) Å, with the order Pt−P bonds *trans* to metal−metal bond > Pt−P bonds *trans* to sulfur > Pt−P bonds *trans* to oxygen being consistent with the previous observation.

Table 3. Selected Bond Lengths (Å) and Angles (deg) for 5

Pt(1)−Pt(2)	3.254(2)	Pt(2)−Pt(3)	3.143(2)
Pt(1)−Pt(3)	3.157(2)	Pt(1)−Re(1)	3.132(2)
Pt(1)−P(1)	2.243(7)	Pt(1)−P(6)	2.244(7)
Pt(2)−P(2)	2.270(7)	Pt(2)−P(3)	2.252(7)
Pt(3)−P(4)	2.231(7)	Pt(3)−P(5)	2.285(7)
Pt(2)−S(1)	2.355(7)	Pt(3)−S(1)	2.329(7)
Re(1)−S(1)	2.516(7)	Pt(1)−O(1)	2.03(1)
Pt(1)−O(2)	2.06(2)	Pt(2)−O(1)	2.02(1)
Pt(3)−O(2)	2.06(2)	Re(1)−O(1)	2.15(1)
Re(1)−O(2)	2.18(2)	Re(1)−C(1)	1.83(3)
Re(1)−C(2)	1.90(3)	Re(1)−C(3)	1.87(3)
O(1)−Pt(1)−O(2)	81.5(6)	O(1)−Pt(1)−P(1)	86.2(5)
O(2)−Pt(1)−P(1)	167.7(5)	O(1)−Pt(1)−P(6)	169.3(5)
O(2)−Pt(1)−P(6)	88.2(5)	P(1)−Pt(1)−P(6)	104.1(3)
O(1)−Pt(1)−Re(1)	42.9(4)	O(2)−Pt(1)−Re(1)	43.8(4)
P(1)−Pt(1)−Re(1)	124.6(2)	P(6)−Pt(1)−Re(1)	126.6(2)
O(1)−Pt(1)−Pt(3)	81.8(4)	O(2)−Pt(1)−Pt(3)	40.0(4)
P(1)−Pt(1)−Pt(3)	138.2(2)	P(6)−Pt(1)−Pt(3)	92.1(2)
Re(1)−Pt(1)−Pt(3)	66.87(4)	O(1)−Pt(1)−Pt(2)	36.6(4)
O(2)−Pt(1)−Pt(2)	81.5(4)	P(1)−Pt(1)−Pt(2)	88.8(2)
P(6)−Pt(1)−Pt(2)	144.4(2)	Re(1)−Pt(1)−Pt(2)	63.84(4)
Pt(3)−Pt(1)−Pt(2)	58.69(3)	O(1)−Pt(2)−P(3)	169.2(5)
O(1)−Pt(2)−P(2)	84.1(5)	P(3)−Pt(2)−P(2)	105.4(3)
O(1)−Pt(2)−S(1)	84.7(5)	P(3)−Pt(2)−S(1)	85.0(3)
P(2)−Pt(2)−S(1)	164.7(3)	O(1)−Pt(2)−Pt(3)	82.2(4)
P(3)−Pt(2)−Pt(3)	93.3(2)	P(2)−Pt(2)−Pt(3)	140.3(2)
S(1)−Pt(2)−Pt(3)	47.5(2)	O(1)−Pt(2)−Pt(1)	36.7(4)
P(3)−Pt(2)−Pt(1)	146.2(2)	P(2)−Pt(2)−Pt(1)	88.7(2)
S(1)−Pt(2)−Pt(1)	88.5(2)	Pt(3)−Pt(2)−Pt(1)	59.11(3)
O(2)−Pt(3)−P(4)	170.6(5)	O(2)−Pt(3)−P(5)	88.5(5)
P(4)−Pt(3)−P(5)	100.4(3)	O(2)−Pt(3)−S(1)	82.8(5)
P(4)−Pt(3)−S(1)	88.7(3)	P(5)−Pt(3)−S(1)	168.0(3)
O(2)−Pt(3)−Pt(2)	84.3(4)	P(4)−Pt(3)−Pt(2)	86.9(2)
P(5)−Pt(3)−Pt(2)	139.2(2)	S(1)−Pt(3)−Pt(2)	48.2(2)
O(2)−Pt(3)−Pt(1)	40.0(4)	P(4)−Pt(3)−Pt(1)	136.7(2)
P(5)−Pt(3)−Pt(1)	87.3(2)	S(1)−Pt(3)−Pt(1)	91.4(2)
Pt(2)−Pt(3)−Pt(1)	62.20(3)	C(1)−Re(1)−C(3)	86.7(14)
C(1)−Re(1)−C(2)	86.3(13)	C(3)−Re(1)−C(2)	85.4(13)
C(1)−Re(1)−O(1)	97.2(11)	C(3)−Re(1)−O(1)	176.0(10)
C(2)−Re(1)−O(1)	94.7(10)	C(1)−Re(1)−O(2)	170.6(11)
C(3)−Re(1)−O(2)	99.8(10)	C(2)−Re(1)−O(2)	100.9(10)
O(1)−Re(1)−O(2)	76.3(6)	C(1)−Re(1)−S(1)	96.0(10)
C(3)−Re(1)−S(1)	101.3(10)	C(2)−Re(1)−S(1)	172.9(10)
O(1)−Re(1)−S(1)	78.4(4)	O(2)−Re(1)−S(1)	76.2(4)
C(1)−Re(1)−Pt(1)	135.2(10)	C(3)−Re(1)−Pt(1)	136.1(9)
C(2)−Re(1)−Pt(1)	85.2(9)	O(1)−Re(1)−Pt(1)	40.1(4)
O(2)−Re(1)−Pt(1)	40.9(4)	S(1)−Re(1)−Pt(1)	88.5(2)
Pt(3)−S(1)−Pt(2)	84.3(2)	Pt(3)−S(1)−Re(1)	91.2(2)
Pt(2)−S(1)−Re(1)	87.8(2)	Pt(2)−O(1)−Pt(1)	106.7(7)
Pt(2)−O(1)−Re(1)	108.1(6)	Pt(1)−O(1)−Re(1)	97.1(6)
Pt(3)−O(2)−Pt(1)	100.0(7)	Pt(3)−O(2)−Re(1)	109.7(7)
Pt(1)−O(2)−Re(1)	95.3(6)	O(3)−C(1)−Re(1)	168(3)
O(4)−C(2)−Re(1)	171(3)	O(5)−C(3)−Re(1)	176(3)

Table 4. Comparison of Metal−Metal Distances (Å) and Unit Cell Volumes (Å³) in 1, 10, 4, 3, and 5[a]

	1	**10**	**4**	**3**	**5**
μ_3 atoms	none	O,O	O,S	S,S	O,O,S
Pt(1)−Pt(2)	**2.611(1)**	**2.826(1)**	**2.957(1)**	**3.038(2)**	3.254(2)
Pt(1)−Pt(3)	**2.593(1)**	3.094(1)	3.152(1)	3.270(2)	3.157(2)
Pt(2)−Pt(3)	**2.608(1)**	3.081(1)	3.115(1)	3.213(2)	3.143(2)
Pt(1)−Re	**2.684(1)**	**2.843(1)**	**2.882(1)**	**2.946(2)**	3.132(2)
Pt(2)−Re	**2.649(1)**	**2.854(1)**	**3.051(1)**	**3.002(2)**	3.378(2)
Pt(3)−Re	**2.685(1)**	3.228(1)	3.426(1)	3.625(2)	3.465(2)
cell vol	*b*	7851(1)	8002(2)	8224(3)	8005(3)

[a] Those distances where a metal−metal bond is proposed are shown in boldface. The accepted range for Pt−Pt-bonded distances is 2.6−2.8 Å; previous values for Pt−Re-bonded distances fall in the range 2.71−2.91 Å, with almost half in the range 2.83−2.87 Å.[3−8] [b] The structure was determined as the BPh_4 salt.

The structure of **5** is different from those of **3** and **4**, since all three Pt_2Re faces of the Pt_3Re cluster contains

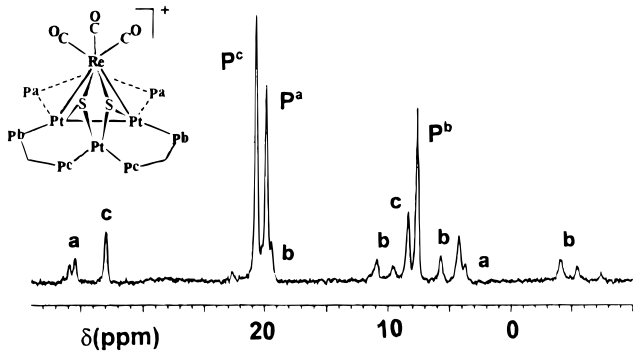

Figure 5. ^{31}P NMR spectrum (121.5 MHz) of complex **3**.

a capping oxo or sulfido ligand. The incorporation of two μ_3-O ligands and one μ_3-S ligand is accompanied by a significant lengthening of all the metal−metal distances compared to those in **1** and even those in **3**, **4**, and **10** (Table 4). The Pt···Re distances of 3.132(2), 3.378(2), and 3.465(2) Å are too long for significant bonding, as are the Pt···Pt distances of 3.254(2), 3.157(2), and 3.143(2) Å. Therefore, the rhenium atom may be considered to have an octahedral geometry with *fac*-$Re(O)_2(S)(CO)_3$ coordination, while each platinum atom has square-planar geometry with *cis*-PtO_2P_2 or *cis*-$PtOSP_2$ coordination. As expected, the Pt−P bonds *trans* to oxygen (Pt−P = 2.231(7)−2.252(7) Å) are shorter than those *trans* to sulfur (2.270(7) and 2.285(7) Å). The Pt−O bond distances (2.02(1)−2.06(2) Å) are similar to the value Pt−O = 2.049(6) Å in **10** and is in the normal range Pt−O distances.[17] There is no disorder of the oxo and sulfido ligands in either **4** or **5**.

Characterization of the Sulfido Clusters by Spectroscopic Methods. The IR spectra of the rhenium tricarbonyl complexes generally contained three terminal carbonyl bands with similar values of ν(CO), as in the parent cluster **1**.[3] This is rationalized if the bridging sulfur or oxygen atom addition reactions lead to formal oxidation at platinum, while the oxidation state at rhenium remains at +I throughout.

The ^{1}H NMR spectra of the new clusters are all consistent with the proposed structures and require little comment. For example, the ^{1}H NMR spectrum in the CH_2P_2 region of **3** shows four broad resonances at 6.54, 4.85, 4.00, and 3.53 ppm in the ratio 1:1:2:2, consistent with the presence of dppm ligands in two different chemical environments in a 2:1 ratio and with the protons of each CH^aH^b group being nonequivalent.

The ^{31}P NMR spectra of the complexes are useful in defining both the cluster symmetry and the presence or absence of Pt−Pt bonds.[18] For example, the spectrum of **3** contains three resonances due to the nonequivalent phosphorus atoms P^a, P^b, and P^c (Figure 5), each with satellites due to $^1J(^{195}Pt^{31}P)$ couplings. This is as expected, since the structure of **3** (Figure 2), in idealized form, has a plane of symmetry containing the atoms Pt(3), Re, and C(1). Long-range couplings $^2J(Pt^1P^b)$ and $^3J(P^bP^b)$ = 167 Hz are observed and indicate the presence of an approximately linear P−Pt−Pt−P unit containing a metal−metal bond. The corresponding long-range couplings ^2J(PtP) and $^3J(P^aP^c)$ are not observed in the multiplets assigned for P^a and P^c, indicating that there is no Pt−Pt bond connecting P^a and P^c. The spectrum therefore supports the conclusion from the structure determination in terms of the distribution of Pt−Pt bonds in **3**, and it is then possible to use the ^{31}P NMR spectra to deduce the structures of related complexes.

The ^{31}P NMR spectrum of the oxo−sulfido cluster **4** is more complex, since there is no plane of symmetry, and so all six dppm phosphorus atoms are nonequivalent. In agreement, six resonances were observed in the ^{31}P NMR spectrum. The assignments were made on the basis of the pattern of coupling constants due to ^1J(PtP), ^2J(PtP), and ^3J(PP). For example, the values of ^1J(PtP) follow the series ^1J(PtP) *trans* to oxygen > ^1J(PtP) *trans* to sulfur > ^1J(PtP) *trans* to a Pt−Pt bond, while large values of ^2J(PtP) and ^3J(PP) are observed only when the coupling occurs through a Pt−Pt bond.

Complex **2** was fluxional at room temperature, and so NMR spectra were also obtained at low temperature down to −90 °C in CD_2Cl_2 solution. The ^{1}H NMR spectrum of **14** at room temperature displays two broad resonances at δ 6.21 and 4.69 in the ratio 1:1. The ^{31}P NMR spectrum at room temperature shows a singlet resonance at δ 3.17 with satellites due to ^1J(PtP) = 2700 Hz. Clearly, all six phosphorus atoms of the μ-dppm ligands are effectively equivalent on the NMR time scale, and this is interpreted in terms of fast rotation of the $\{Re(CO)_3S\}$ unit around the Pt_3 triangle. The observation of long-range couplings ^2J(PtP) = 600 Hz and ^3J(PP) = 170 Hz indicates the presence of Pt−Pt bonds in **2**. At −90°C, the ^{31}P NMR spectrum contained six broad resonances due to six nonequivalent dppm phosphorus atoms, indicative of low symmetry for the cluster cation of **2**; the coalescence temperature was *ca.* −60 °C. These data are consistent with the proposed structure of **2**, with the terminal Re═S group in a low-symmetry conformation, but not with the alternative structure $[Pt_3\{Re(CO)_3\}(\mu_3\text{-}S)(\mu\text{-dppm})_3]^+$. Thus, a μ_3-S group would surely prevent rotation of the $Re(CO)_3S$ group needed to give the observed fluxionality, just as the bridging oxo ligand prevents fluxionality in cluster **9**. Terminal Re═S groups are well-known, and examples are found in the complexes $[(S_4)_2ReS]^-$ and $[ReS_4]^-$, but, of course, triply bridging sulfide ligands are also common, for example in the structure of ReS_2.[19,20] Further evidence that the first sulfidation occurs at rhenium is found by comparing the XPS binding energies for **1**−**3**. The following energies (eV) are for the Re $4f_{7/2}$ and Pt $4f_{7/2}$ levels: **1**, 41.6 and 72.6; **2**, 42.0 and 72.9; **3**, 41.7 and 73.0. The sequence of Re $4f_{7/2}$ binding energies **2** > **3** > **1** suggests that the first sulfidation leads to formal oxidation at rhenium in forming **2**.

The ^{31}P NMR spectrum of $[Pt_3\{Re(CO)_3S\}(\mu_3\text{-}O)(\mu\text{-dppm})_3][PF_6]$ (**7**$[PF_6]$), is complex but quite different from that of its isomer **4**. There are six resonances,

(17) Betz, P.; Bino, A. *J. Am. Chem. Soc.* **1988**, *110*, 602.

(18) (a) Powell, J.; Sawyer, J. F.; Stainer, M. V. R. *Inorg. Chem.*, **1989**, *28*, 4461. (b) Bao, Q.-B.; Geib, S. J.; Rheingold, A. L.; Brill, T. B. *Inorg. Chem.* **1987**, *26*, 3453. (c) Mather, G. G.; Pidcock, A.; Rapsey, G. J. N. *J. Chem. Soc., Dalton Trans.* **1973**, 2095. (d) Pidcock, A. *Adv. Chem. Ser.* **1982**, *No. 196*, 1.

(19) (a) Müller, A.; Krickemeyer, E.; Bogge, H.; Penk, M.; Rehder, D. *Chimia* **1986**, *40*, 50. (b) Muller, A.; Diemann, E.; Jostes, R.; Bogge, H. *Angew. Chem., Int. Ed. Engl.* **1981**, *20*, 934. (c) Muller, A.; Diemann, E.; Rao, V. V. K. *Chem. Ber.* **1970**, *103*, 2961.

(20) Murray, H. H.; Kelty, S. P.; Chianelli, R. R.; Day, C. S. *Inorg. Chem.* **1994**, *33*, 4418.

(21) (a) Puddephatt, R. J.; Manojlovic-Muir, L.; Muir, K. W. *Polyhedron* **1990**, *9*, 2767. (b) Imhof, D.; Venanzi, L. M. *Chem. Soc. Rev.* **1994**, 185.

indicating low symmetry. Two singlet resonances at δ −9.9 and −10.1 can be readily assigned to phosphorus atoms *trans* to oxygen on the basis of the large ^1J(PtP) coupling constants of 3880 and 3856 Hz, respectively, demonstrating the presence of a μ_3-O group. Assignment of the other four resonances is based on the pattern of couplings to these phosphorus atoms and is tentative. These data are insufficient to define the structure, but since the complex clearly has a different structure from that of **4** and since the precursor very likely contains a terminal Re═S group, the structure **7** appears most reasonable and is consistent with the spectroscopic data. The structural conclusion is tentative in this case.

The ^{31}P NMR spectra of **5** and **8** each contain three singlet resonances with $^1J(^{195}Pt^{31}P)$ satellites. Since these compounds contain no Pt−Pt bonds, there are no long-range couplings ^2J(PtP) or ^3J(PP). The phosphorus atoms *trans* to oxygen have larger values of ^1J(PtP) than do those *trans* to sulfur.

The ^{31}P NMR spectrum of cluster **6** contained three resonances and was similar to that of **3**. Of course, the IR spectrum of **6** contains no carbonyl bands but contains a strong band at ν(Re═O) = 906 cm^{-1} due to the ReO_3 fragment; the value of ν(Re═O) in **6** is similar to that in the precursor $[Pt_3\{ReO_3\}(\mu\text{-dppm})_3]^+$ (**12**; 904 cm^{-1}).

Discussion

These bimetallic Pt−Re clusters containing sulfur or both sulfur and oxygen ligands provide the first molecular bimetallic cluster models for the structure and nature of presulfided and sulfided supported Pt−Re bimetallic catalysts, which are important as petroleum re-forming catalysts. The reaction of propylene sulfide with the coordinatively unsaturated cluster cation $[Pt_3\{Re(CO)_3\}(\mu\text{-dppm})_3]^+$ (**1**) occurs under very mild conditions to give the sulfido clusters $[Pt_3\{Re(CO)_3S\}(\mu\text{-dppm})_3]^+$ (**2**) and $[Pt_3\{Re(CO)_3\}(\mu_3\text{-S})_2(\mu\text{-dppm})_3]^+$ (**3**) without loss of any ligands. That organic episulfides can act as sulfur-transfer agents was already known,[9,22] but there are few known reactions in which sulfido transition-metal clusters have been formed by the use of episulfides, and these occur with displacement of ligands by sulfide.[9,23,24] The addition of the two sulfur atoms to **1** to form **3** leads to an increase in the cluster electron count from 54 to 62 electrons and results in loss of metal−metal bonding. Although the metal−metal distances Pt(1)−Pt(2) = 3.038(2) Å, Pt(1)−Re = 2.946(2) Å, and Pt(2)−Re = 3.002(2) Å are longer than those in **1**, there is still evidence for metal−metal bonding within the Pt(1)Pt(2)Re triangle. The observation of long-range couplings ^2J(PtP) = 632 Hz and ^3J(PP) = 175 Hz across the Pt(1)−Pt(2) bond confirms this conclusion.[10,25] According to the simple bonding model shown in Chart 1, the bonding in **3** may be illustrated in terms of two 16-electron Pt(I) atoms, Pt-

Chart 1

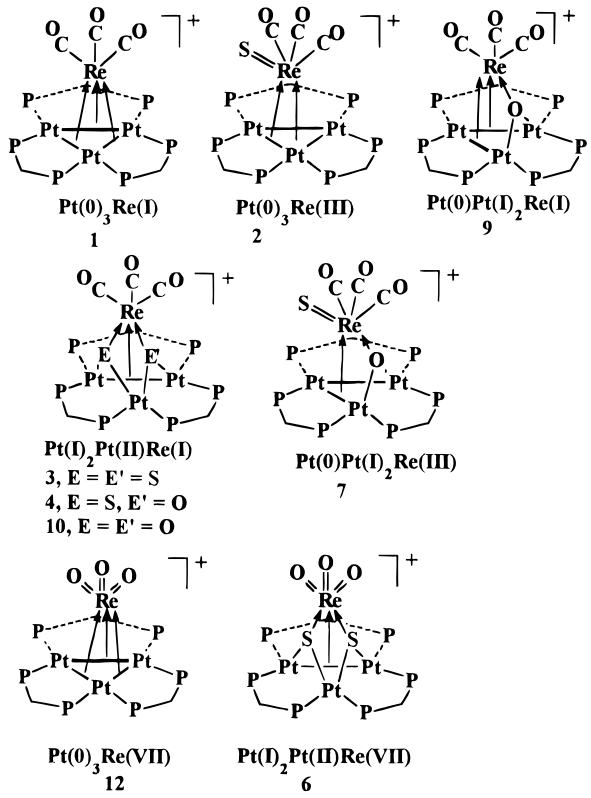

(1) and Pt(2), having similar distorted-square-planar *cis*-$PtSP_2Pt$ environments with a Pt(1)−Pt(2) bond, a square-planar 16-electron Pt(II) atom, Pt(3), with a *cis*-PtS_2P_2 center, and an octahedral *fac*-$Re^I(S)_2(CO)_3$ center in which rhenium can achieve an 18-electron configuration by accepting 2 electrons from the Pt(1)−Pt(2) bond and 2 electrons from each sulfur atom. Thus, the formal metal oxidation states in **3** may be considered to be $Pt^I_2Pt^{II}Re^I$. Besides the dioxo analogue **10** and the monooxo monosulfido analog **4**, clusters which are structurally related to **3** include $[Os_4(CO)_{12}(\mu_3\text{-S})_2]$[24,26] and $[Os_3W(CO)_{12}(PMe_2Ph)(\mu_3\text{-S})_2]$,[24,27] and they can readily react with 2-electron-donor ligands CO and PMe_2Ph to form adducts.[24] In contrast, complex **3** is rather stable and does not react with either σ-donor or π-acceptor ligands under mild conditions. In particular, it does not undergo the type of ligand substitution reaction found for the dioxo analog **10**.

Since both clusters **1** and **12** have 54-electron counts and similar metal−metal bonding, and since both clusters **3** and **6** have 62-electron counts, it is reasonable to expect a pattern of metal−metal bonding in **6** similar to that established in **3**. However, the oxidation states in cluster **6** may be considered to be $Pt^I_2Pt^{II}Re^{VII}$ (Chart 1). This formulation is fully consistent with the spectroscopic data.

The highest cluster electron counts of 66e are observed for the dioxo sulfido and the oxo disulfido clusters **5** and **8**, respectively. The structure of **5** confirms that all platinum atoms have square-planar stereochemistry[28,29] while rhenium has octahedral stereochemistry

(22) Linford, L.; Raubenheimer, H. G. *Adv. Organomet. Chem.* **1991**, *32*, 1.
(23) (a) King, R. B. *Inorg. Chem.* **1963**, *2*, 326. (b) Dahl, L. F.; Sutton, P. W. *Inorg. Chem.* **1963**, *2*, 1067. (c) Havlin, R.; Knox, G. R. *J. Organomet. Chem.* **1965**, *4*, 247.
(24) Albers, M. O.; Robinson, D. J. *Coord. Chem. Rev.* **1986**, *69*, 127.
(25) Boag, N. M.; Browning, J.; Crocker, C.; Goggin, P. L.; Goodfellow, R. J.; Murray, M.; Spencer, J. L. *J. Chem. Res., Synop.* **1978**, 228; *J. Chem. Res., Miniprint* **1978**, 2962.
(26) Adams, R. D.; Yang, L.-W. *J. Am. Chem. Soc.* **1983**, *105*, 235
(27) Adams, R. D.; Horvath, I. T.; Mathur, P. *J. Am. Chem. Soc.* **1984**, *106*, 6296.
(28) Collman, J. P.; Hegedus, L. S.; Norton, J. R.; Finke, R. G. *Principles and Applications of Organotransition Metal Chemistry*; University Science Books: Mill Valley, CA, 1987.

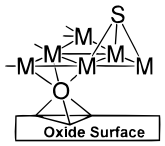

Figure 6. Possible structure of a sulfided Pt−Re catalyst on an oxide support. The atoms M may be platinum or rhenium. It is likely that the more oxophilic rhenium may be concentrated at the oxide interface, with exposed rhenium atoms also being sulfided.

and that no metal−metal bonding is present. The Re center adopts an octahedral geometry in which rhenium has an 18-electron configuration. Thus, the structures are consistent with the predictions of the Wade-Mingos rules,[30] adapted for platinum having a 16-electron count. For these complexes, the metal oxidation states are considered to be $Pt^{II}_3Re^{I}$, (Chart 1).

The greatest uncertainty concerns the structure and bonding in the clusters **2** and **7**, which are proposed to have terminal Re═S groups. For **2** the main evidence comes from the observation of fluxionality, which is not expected for a cluster with a bridging sulfido ligand, while for **7** the structural conclusion is based on the major differences in NMR parameters compared to the structurally characterized complex **4**. We have not succeeeded in growing crystals of either **2** or **7** of diffraction quality. Hence, the structural conclusions are tentative. If they are correct, the electron counts would be 56e and 60e and the oxidation states $Pt^{0}_3Re^{III}$ and $Pt^{I}_2Pt^{0}Re^{III}$ for **2** and **7** respectively.

In terms of the cluster−surface analogy, the formation of the series of sulfide cluster complexes discussed above can be thought to mimic the sulfidation of supported Pt−Re catalysts. It can be predicted that the sulfidation of these catalysts will probably occur initially at rhenium but that the sulfide is likely to be most stable as a surface μ_3-S ligand with $Pt_2Re(\mu_3\text{-}S)$ groups. In this way a surface sulfide is likely to deactivate toward catalysis not only the surface rhenium atoms but also the immediately adjacent surface platinum atoms, so rationalizing the observed sulfur effect on the Pt−Re catalysts at low sulfur coverage.[3,31] Therefore, this model system supports and adds new detail to the current interpretation on the role of sulfidation in supported Pt−Re catalysts. Considering that the Pt−Re catalysts are supported on the surface of oxide supports, the structure of the sulfided supported Pt−Re catalysts may be depicted as shown in Figure 6. The oxygen atoms from the oxide support may also likely function as surface μ_3-O ligands, and the metals are simultaneously singly bonded to several oxygen atoms in the oxide surface, while the sulfur atoms are bonded on the other faces of the Pt−Re clusters in a μ_3 bonding mode and thus a $Pt_2(\mu_3\text{-}O)Re(\mu_3\text{-}S)$ unit is formed. A similar surface oxygen−metal bonding structure has been proposed for mononuclear metal catalysts on oxide supports on the basis of EXAFS studies.[32] It has been found that a metal-oxygen distance of about 2.1 Å is characteristic of second- and third-row transition metals that are present in low positive oxidation states and are singly bonded to oxygen on the basis of the study of surface catalysts,[32a] in the same range as the values found for **3**−**5**. The Pt_3Re cluster clusters described in this paper thus provide good models for the structure and bonding in sulfided oxide-supported Pt−Re catalysts. Of course, further proof is needed and must be obtained from the direct study of Pt−Re catalysts.

Experimental Section

General methods and the synthesis of starting materials have been described previously.[3−5] In NMR data, all δ values are in units of ppm and J values in Hz.

$[Pt_3\{Re(CO)_3S\}(\mu\text{-dppm})_3][PF_6]$ (2[PF$_6$]). This experiment was carried out several times, and a typical experiment is described. To a solution of $[Pt_3\{Re(CO)_3\}(\mu\text{-dppm})_3][PF_6]$ (32 mg, 0.015 mmol) in CH_2Cl_2 (15 mL) was added propylene sulfide (1.2 μL, 0.015 mmol) via microsyringe with stirring. The reaction was monitored by ^{1}H and ^{31}P NMR spectroscopy; it took about 0.5 h to reach completion. The solution was then concentrated to *ca*. 2 mL under vacuum. Complex **2** was precipitated with diethyl ether (15 mL) followed by vacuum drying to give the product as a yellow-brown powder in 90% yield. Anal. Calcd for $C_{78}H_{66}F_6O_3P_7Pt_3ReS\cdot CH_2Cl_2$: C, 41.79; H, 3.02. Found: C, 41.86; H, 2.89. IR (Nujol): ν(CO) 1979 (s), 1874 (s), 1850 (sh) cm^{-1}. NMR (CD_2Cl_2): ^{1}H, δ 6.21 [br, 3H, H^aCP_2], 4.69 [br, 3H, H^bCP_2]; ^{31}P{^{1}H}, δ 4.0 [s, 6P, ^1J(PtP) = 2700, ^2J(PtP) = 600, ^3J(PP) = 170, dppm]; ^{31}P{^{1}H} at −90 °C, δ −16, −11, −7.7, −5, 6.3, 8.5 [m, dppm]; ^{31}P{^{1}H} at −60 °C, δ −3.1 (br), at coalescence temperature.

$[Pt_3\{Re(CO)_3\}(\mu_3\text{-}S)_2(\mu\text{-dppm})_3][PF_6]$ (3[PF$_6$]). To a solution of **1** (87 mg, 0.04 mmol) in acetone (25 mL) was added propylene sulfide (10 μL) via microsyringe. The dark brown solution changed to red in 5 min. After 2 h of stirring, the solution was concentrated, followed by addition of hexane to give a precipitate of complex **3**, which was further washed with hexane. A reddish crystalline product was obtained. Well-shaped red prismatic crystals could be obtained from acetone/hexane. Yield: 95%. Anal. Calcd for $C_{78}H_{66}F_6O_3P_7Pt_3ReS_2$: C, 42.24; H, 3.00. Found: C, 42.36; H, 2.92. IR (Nujol): ν(CO) 1979 (s), 1885 (s), 1863 (s) cm^{-1}. NMR (CD_2Cl_2): ^{1}H, δ 6.54 [br, 1H, H^aCP_2], 4.85 [m, 1H, H^bCP_2], 4.00 [br, 2H, $H^{a'}CP_2$], 3.53 [br, 2H, $H^{b'}CP_2$]; ^{31}P{^{1}H}, δ 15.6 [m, 2P^c, ^1J(PtP^c) = 2987, dppm], 14.8 [m, 2P^a, ^1J(PtP^a) = 3850, ^2J(P^{a}P^a) = 57, dppm], 2.6 [m, 2P^b, ^1J(PtP^b) = 3038, ^2J(PtP^b) = 632, ^3J(P^{b}P^b) = 167, dppm].

$[Pt_3\{Re(CO)_3S\}(\mu_3\text{-}O)(\mu\text{-dppm})_3][PF_6]$ (7[PF$_6$]). To a solution of **2** (31 mg, 0.016 mmol) in CH_2Cl_2 (15 mL) was added Me_3NO (1.1 mg). After 4 h of stirring, a reddish solution formed, which was then concentrated to *ca*. 2 mL followed by precipitating with hexane, and the precipitate was further washed with diethyl ether to give the product as a yellow-brown powder. Well-shaped red prismatic crystals could be obtained from CD_2Cl_2/hexane. Yield: 70%. Anal. Calcd for $C_{78}H_{66}F_6O_4P_7Pt_3ReS$: C, 42.55; H, 3.02. Found: C, 42.65; H, 3.25. IR (Nujol): ν(CO) 1979 (s), 1876 (sh), 1868 (s) cm^{-1}. NMR (CD_2Cl_2): ^{1}H, δ 6.65 [m, 2H, $H^aH^{a'}CP_2$], 6.19 [m, 2H, $H^bH^{b'}$-CP_2], 3.73 [m, 2H, $H^cH^{c'}CP_2$]; ^{31}P{^{1}H}, δ 27.4 [quin, 1P^e, ^1J(PtP) =2992, dppm], 22.8 [quin, 1P^f, ^1J(PtP) = 2786, dppm], 8.3 [t, 1P^b, ^1J(PtP) = 3112, dppm], 4.8 [t, 1P^c, ^1J(PtP) = 3042, dppm], −9.9 [m, 1P^a, ^1J(PtP) = 3880, dppm], −10.1 [m, 1P^d, ^1J(PtP) = 3856, dppm].

$[Pt_3\{Re(CO)_3\}(\mu_3\text{-}O)(\mu_3\text{-}S)(\mu\text{-dppm})_3][PF_6]$ (4[PF$_6$]). To a solution of **1** (35 mg, 0.016 mmol) in CD_2Cl_2 (0.5 mL) in an NMR tube was added Me_3NO (1.2 mg). The solution was shaken vigorously until all Me_3NO dissolved. One hour later,

(29) (a) Evans, D. G. *J. Organomet. Chem.* **1988**, *352*, 397. (b) Mealli, C. *J. Am. Chem. Soc.* **1985**, *107*, 2245.

(30) Mingos, D. M. P.; Wales, D. J. *Introduction to Cluster Chemistry*; Prentice-Hall: Englewood Cliffs, NJ, 1990.

(31) (a) Van Trimpont, P. A.; Marin, G. B.; Froment, G. F. *Appl. Catal.* **1985**, *17*, 161. (b) Biloen, P.; Helle, J. N.; Verbeek, H.; Dautzenberg, F. M.; Sachtler, W. H. M. *J. Catal.* **1980**, *63*, 112. (c) Coughlin, R. W.; Hasan, A.; Kawakami, K. *J. Catal.* **1984**, *88*, 163.

(32) (a) Chang, J.-R.; Gron, L. U.; Honji, A.; Sanchez, K. M.; Gates, B. C. *J. Phys. Chem.* **1991**, *95*, 9944. (b) Day, V. W.; Klemperer, W. G.; Main, D. J. *Inorg. Chem.* **1990**, *29*, 2345.

^{31}P NMR monitoring showed that the reaction was complete, with complexes $[Pt_3\{Re(CO)_3\}(\mu_3\text{-}O)(\mu\text{-}dppm)_3]^+$ (**9**) and $[Pt_3\{Re(CO)_3\}(\mu_3\text{-}O)_2(\mu\text{-}dppm)_3]^+$ (**10**) being formed in the ratio 5:1. There was no obvious color change at this stage. Then, propylene sulfide (2.5 μL) was added. The solution became red immediately. ^{31}P NMR monitoring showed that the reaction was complete in 12 h. The product was precipitated with hexane to give an orange powder. Well-shaped red crystals of **4** could be obtained from CH_2Cl_2/hexane. Yield: 50%. Anal. Calcd for $C_{78}H_{66}F_6O_4P_7Pt_3ReS$: C, 42.55; H, 3.02. Found: C, 42.60; H, 3.12. IR (Nujol): ν(CO) 1978 (s), 1877 (sh), 1860 (s) cm^{-1}. NMR (CD_2Cl_2): ^{1}H, δ 4.82 [m, 1H, H^a CP$_2$], 4.00 [m, 1H, H^b CP$_2$], 3.69 [m, 1H, $H^{a'}$ CP$_2$], 3.56 [m, 1H, $H^{b'}$ CP$_2$], 3.31 [m, 1H, H^c CP$_2$], 2.92 [m, 1H, $H^{c'}$ CP$_2$]; ^{31}P{^{1}H}, δ 17.1 [m, 1P^c, ^1J(PtP) =3285, dppm], 9.6 [dm, 1P^a, ^1J(PtP^a) = 3920, ^2J(P^{a}P^f) = 47, dppm], 5.2 [m, 1P^d, ^1J(PtP) = 3184, dppm], 3.8 [dm, 1P^f, ^1J(PtP) = 3777, ^2J(P^{a}P^f) = 47, dppm], 2.0 [dm, 1P^e, ^1J(PtP^e) = 3075, ^2J(PtP^e) = 1166, ^3J(P^{b}P^e) = 175, dppm], 0.3 [dm, 1P^b, ^1J(PtP^b) = 3054, ^2J(PtP^b) = 680, ^3J(P^{b}P^e) = 175, dppm].

$[Pt_3\{Re(CO)_3\}(\mu_3\text{-}O)_2(\mu_3\text{-}S)(\mu\text{-}dppm)_3][PF_6]$ (5[PF$_6$]). To a solution of **10** (45 mg, 0.021 mmol) in CH_2Cl_2 (15 mL) was added propylene sulfide (3 μL). The orange solution changed to bright yellow in 20 min. The mixture was stirred for 4 h. The solution was then concentrated to 2 mL. Hexane was added to precipitate the product, which was further washed with hexane followed by vacuum drying to give the product as bright yellow crystals in 98% yield. Well-shaped bright yellow prismatic crystals could be obtained from CH_2Cl_2/diethyl ether. Anal. Calcd for $C_{78}H_{66}F_6O_5P_7Pt_3ReS\cdot{}^1/_2CH_2Cl_2$: C, 41.72; H, 2.99. Found: C, 41.90; H, 2.84. IR (Nujol): ν(CO) 1989 (vs), 1865 (sh), 1856 (vs) cm^{-1}. NMR (CD_2Cl_2): ^{1}H, δ 3.61 [m, 1H, H^a CP$_2$], 3.41 [m, 1H, H^b CP$_2$], 2.91 [br, 2H, $H^{a'}$ CP$_2$], 2.25 [br, 2H, $H^{b'}$ CP$_2$]; ^{31}P{^{1}H}, δ 14.62 [m, 2P^b,^1J(PtP) =3190, dppm], 0.70 [m, 2P^c, ^1J(PtP) = 3283, dppm], 0.83 [br, 2P^a, ^1J(PtP) = 3388, dppm].

$[Pt_3\{Re(CO)_3\}(\mu_3\text{-}O)(\mu_3\text{-}S)_2(\mu\text{-}dppm)_3][PF_6]$ (8[PF$_6$]). To a solution of **3** (36 mg, 0.016 mmol) in CH_2Cl_2 (50 mL) was added H_2O_2/ H_2O (0.8 mL, *ca*. 30%). After 4 h of stirring, the solution became lighter in colour. The mixture was stirred overnight. Distilled water was then added several times to remove the unreacted H_2O_2 until the organic layer became clear. The CH_2Cl_2 solution was then separated from the H_2O layer and concentrated to 2 mL. Hexane was added to precipitate the product, which was then dried under vacuum to afford an orange product which, by integration of the ^{31}P NMR, was composed of about 50% **8** and 50% $CH_2(POPh_2)_2$. IR (Nujol): ν(CO) 1980 (s), 1889 (s), 1861 (s) cm^{-1}. NMR ($(CD_3)_2CO$): ^{31}P{^{1}H}, δ 18.8 [s, 2P^a, ^1J(PtP) = 3233, dppm], 14.0 [s, 2P^c, ^1J(PtP) = 3156, dppm], −5.1 [s, 2P^a, ^1J(PtP) = 3424, dppm].

$[Pt_3\{ReO_3\}(\mu_3\text{-}S)_2(\mu\text{-}dppm)_3][PF_6]$ (6[PF$_6$]). To a stirred solution of $[Pt_3\{ReO_3\}(\mu\text{-}dppm)_3][PF_6]$ (**12**; 34 mg, 0.016 mmol) in CH_2Cl_2 (15 mL) was added propylene sulfide (40 μL) via syringe. The clear red-brown solution became orange-yellow in 0.5 h. After 16 h of stirring, the solution was concentrated to *ca*. 2 mL in vacuo followed by precipitation by hexane to give the product as a brown-yellow oil in 83% yield. IR (Nujol): ν(Re=O) of ReO_3 906 (vs, br) cm^{-1}. NMR (CD_2Cl_2): ^{1}H, δ 5.25 [br, 2H, H^aH^b CP$_2$], 4.28 [br, 4H, $H^{a'}H^{b'}$ CP$_2$]; ^{31}P-{^{1}H}, δ 26.0 [m, 2P^a, ^1J(PtP) = 2647, dppm], 5.6 [m, 2P^b, ^1J(PtP) = 3016, ^2J(PtP^b) = 164, ^3J(P^{b}P^b) = 168, dppm], −5.7 [m, 2P^a, ^1J(PtP^a) = 3962, ^2J(P^{a}P^a) = 41, dppm]. This reaction proceeds via an intermediate, as monitored by ^{31}P NMR spectroscopy. The intermediate could not be isolated, and and its identity is not yet clear. NMR (CD_2Cl_2): ^{31}P{^{1}H}, δ 23.6 [br, 2P, dppm], 7.4 [s, br, 4P, ^1J(PtP) = 3404, dppm].

X-ray Structure Determinations. The crystal densities were measured by the neutral buoyancy method. The crystals were examined in paraffin oil, and the data crystal was wedged inside a Lindemann capillary tube that was flame-sealed. The diffraction experiments were carried out on a Siemens P4 four-circle diffractometer with the XSCANS software package[33] using graphite-monochromated Mo Kα radiation at 27 °C. The cell constants were obtained by centering 25−37 high-angle reflections ($12.9 \le 2\theta \le 23.4°$). The Laue symmetry 2/*m* was determined by merging symmetry-equivalent reflections in each case. Data were collected in the θ-2θ scan mode at variable scan speeds (1−10°/min), and background measurements were made at the ends of the scan range. Three standard reflections were monitored at the end of every 297 reflections collected. The data processing, solution, and refinements were done using SHELXTL-PC programs.[34] The final refinements on F^2 for **4** and **5** were performed using SHELX-93 programs.[35] The systematic absences suggested the space group $P2_1/n$ in each case, and this was confirmed by successful solution and refinement. Anisotropic thermal parameters were assigned and refined for Pt, Re, S, P, and O atoms. All the phenyl rings were treated as ideal hexagons with C−C distances of 1.395 Å. No attempt was made to locate the hydrogen atom positions, and all the hydrogen atoms were placed in calculated positions and included for the purpose of structure factor calculations only. A common thermal parameter was assigned for all hydrogen atoms and refined in the least-squares cycles. A summary of experimental and crystal data is given in Table 5, and complete experimental details and tables of crystal data, positional and thermal parameters, bond distances and angles, anisotropic thermal parameters, and hydrogen atom coordinates are included in the Supporting Information.

X-ray Structure Determination for $3\cdot{}^1/_2Me_2CO$. Dark red distorted-pyramidal single crystals were grown by diffusion of hexane into the acetone solution at room temperature. In all, 12 032 reflections were collected in the 2θ range 3.5−45° ($-1 \le h \le 18$, $-1 \le k \le 25$, $-21 \le l \le 21$). The data were corrected for absorption by an empirical method involving ψ scans using 14 reflections ($7.0 < 2\theta < 17.2°$). The maximum and minimum transmission factors were 0.059 and 0.039, respectively. In the PF_6^- anion, the fluorine atoms in the equatorial positions were found to be disordered. Two different orientations of the disordered F atoms were found to be related by a rotation of 45° around the F(1)−P(7)−F(2) axis, and their occupancies (0.6/0.4) were derived from the ratio of their electron densities obtained from the difference Fourier routines. Due to this disorder problem each fragment was treated as an ideal octahedron with P−F distances of 1.45 Å. Individual isotropic thermal parameters were assigned for each fluorine atom and refined in the least-squares cycles. Two fragments of an acetone solvent molecule were located in the crystal lattice,one of which was disordered. The disordered fragments were related by a mirror plane along the methyl carbon atoms. Ideal geometrical constraints were imposed (C−O = 1.20 Å, C−C = 1.54 Å, and C−C−C and C−C−O angles 120°) for the disordered acetone fragments. Common isotropic thermal parameters were assigned and refined in the least-squares cycles. Hydrogen atoms were not included for the solvent molecule.

X-ray Structure Determination for $4\cdot{}^1/_2C_6H_{12}\cdot{}^1/_2CH_2Cl_2$. Red crystals were grown from a dichloromethane/hexane mixture by the diffusion method at room temperature. A total of 12 053 reflections were collected in the θ range 2.0−23.0° ($-1 \le h \le 18$, $-1 \le k \le 25$, $-21 \le l \le 21$). The faces of the data crystal were indexed, and the distances between them were measured and a numerical absorption correction was applied to the data. The maximum and minimum transmission factors were 0.5827 and 0.3721, respectively. The fluorine atoms F(3)−F(6) in the PF_6^- anion were found to be disordered around P(7). The two disorder models were related by a 45°

(33) XSCANS, Siemens Analytical X-Ray Instruments Inc., Madison, WI, 1990.
(34) Sheldrick, G. M. SHELXTL-PC Software, Siemens Analytical X-Ray Instruments Inc., Madison, WI, 1990.
(35) Sheldrick, G. M. SHELX-93, University of Gottingen, Gottingen, Germany, 1993.

Table 5. Crystal Data and Experimental Details for 3−5

	3	4	5
formula	$C_{78}H_{66}F_6O_3P_7Pt_3ReS_2 \cdot C_3H_6O$	$C_{78}H_{66}F_6O_4P_7Pt_3ReS \cdot C_{3.5}H_7Cl$	$C_{82}H_{76}F_6O_6P_7Pt_3ReS \cdot C_4H_{10}O$
fw	1398.59	2301.29	2291.82
T/°C	27	25	25
λ/Å	0.710 73	0.710 73	0.710 73
cryst syst	monoclinic	monoclinic	monoclinic
space group	$P2_1/n$	$P2_1/n$	$P2_1/n$
a/Å	17.321(4)	17.085(2)	17.133(3)
b/Å	23.890(6)	23.531(3)	23.494(4)
c/Å	19.932(3)	19.984(2)	19.976(4)
β/deg	94.36(1)	95.154(7)	95.42(1)
V/Å^3	8224(3)	8002(2)	8005(3)
Z	4	4	4
ρ_c/g cm^{-3}	1.838	1.90	1.902
μ/mm^{-1}	0.65	7.0	6.9
F(000)	4360	4376	4400
no. of rflns	10 580	10 935	11 160
no. of obs rflns ($I > 2\sigma(I)$)	5137	5963	5725
no. of params	341	425	446
R^a	$R = 0.0637$	R1 = 0.0694	R1 = 0.0813
$R_w{}^a$	$R_w = 0.0588$	wR2 = 0.1235	wR2 = 0.1525
GOF^a	1.1172	1.021	1.012

[a] $R1 = \sum(||F_o| - |F_c||)/\sum|F_o|$; $R_w = [\sum(||F_o| - |F_c||)w^{1/2}]/\sum|F_o|w^{1/2}]$; $wR2 = [\sum w(F_o^2 - F_c^2)^2/\sum wF_o^4]^{1/2}$; $GOF = [\sum w(F_o^2 - F_c^2)^2/(n - p)]^{1/2}$, where n is the number of reflections and p is the number of parameters refined.

rotation along the F(1)−P(7)−F(2) axis (occupancies 0.63 and 0.37). Ideal octahedral geometry constraints were imposed and a common P−F length was refined in the least-squares cycles. Common isotropic thermal parameters were refined for each set of fluorine atoms in the least-squares cycles. Half-molecules of hexane and dichloromethane located in the crystal lattice were also disordered. Ideal constraints were imposed (C−C = 1.54 Å, and C−C−C = 109.5° for hexane and C−Cl = 1.65 Å for dichloromethane). Common isotropic thermal parameters were assigned for each solvent and refined. Hydrogen atoms were not included for the solvent molecules. The oxygen atom O(4) of one carbonyl group was found to have two orientations. Both the disordered O(4) positions and their isotropic temperature factors were refined.

X-ray Structure Determination for 5·Et$_2$O. Light yellow platelike crystals were grown from a dichloromethane/diethyl ether mixture by the diffusion method at room temperature. A total of 11 974 reflections were collected in the θ range 1.8−23.0° ($-1 \le h \le 18$, $-1 \le k \le 25$, $-21 \le l \le 21$) in the ω scan mode at variable scan speeds (2−10°/min). The faces of the data crystal were indexed, the distances between them were measured, and a numerical absorption correction was applied to the data. The maximum and minimum transmission factors were 0.728 and 0.459, respectively. The fluorine atoms in the PF_6^- anion were disordered around P(7), in the same sense as in **3**, and were treated in the same way. A common isotropic thermal parameter was refined for each set of fluorine atoms in the least-squares cycles. One molecule of diethyl ether solvate in the crystal lattice was also found to be disordered. Ideal constraints were imposed (C−O = 1.40 Å and C−C = 1.54 Å) for the two disorder models (multiplicity ratio 0.6:0.4). Common isotropic thermal parameters were assigned for each set of disorder fragments and refined. No hydrogen atoms were included for the solvent molecule.

Acknowledgment. We thank the PRF and NSERC of Canada for financial support.

Supporting Information Available: Text giving experimental details of the X-ray structure determinations for **3**−**5** and tables of crystal data, positional and thermal parameters, bond distances and angles, anisotropic thermal parameters, and hydrogen atom coordinates (31 pages). Ordering information is given on any current masthead page.

OM9610612